ACS Chemical Neuroscience

Research Article

pubs.acs.org/chemneuro

Cellular Polyamines Promote Amyloid-Beta (Aβ) Peptide Fibrillation and Modulate the Aggregation Pathways

Jinghui Luo,[†] Chien-Hung Yu,[†] Huixin Yu,[‡] Rok Borstnar,[§,∥] Shina C. L. Kamerlin,[§] Astrid Gräslund,[⊥] Jan Pieter Abrahams,*[,†] and Sebastian K. T. S. Wärmländer*[,⊥]

[†]Gorlaeus Laboratory, Leiden Institute of Chemistry and [‡]Leiden/Amsterdam Center for Drug Research, Leiden University, 2300RA Leiden, The Netherlands

[§]Department of Cell and Molecular Biology (ICM), Uppsala University, SE-75124 Uppsala, Sweden

[∥]National Institute of Chemistry, Hajdrihova, 19 SI-1001 Ljubljana, Slovenia

[⊥]Department of Biochemistry and Biophysics, Stockholm University, SE-10691 Stockholm, Sweden

Supporting Information

ABSTRACT: The cellular polyamines spermine, spermidine, and their metabolic precursor putrescine, have long been associated with cell-growth, tumor-related gene regulations, and Alzheimer's disease. Here, we show by in vitro spectroscopy and AFM imaging, that these molecules promote aggregation of amyloid-beta (Aβ) peptides into fibrils and modulate the aggregation pathways. NMR measurements showed that the three polyamines share a similar binding mode to monomeric Aβ(1−40) peptide. Kinetic ThT studies showed that already very low polyamine concentrations promote amyloid formation: addition of 10 μM spermine (normal intracellular concentration is ∼1 mM) significantly decreased the lag and transition times of the aggregation process. Spermidine and putrescine additions yielded similar but weaker effects. CD measurements demonstrated that the three polyamines induce different aggregation pathways, involving different forms of induced secondary structure. This is supported by AFM images showing that the three polyamines induce Aβ(1−40) aggregates with different morphologies. The results reinforce the notion that designing suitable ligands which modulate the aggregation of Aβ peptides toward minimally toxic pathways may be a possible therapeutic strategy for Alzheimer's disease.

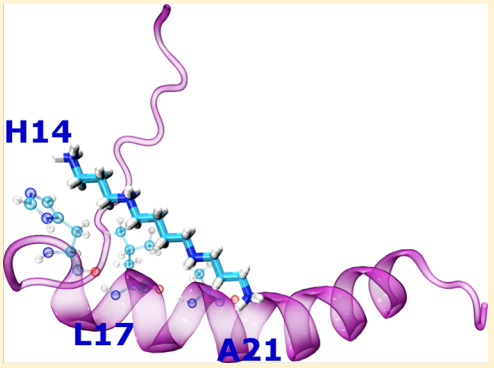

KEYWORDS: *Alzheimer's disease, amyloid-beta peptide, natural polyamines, protein−ligand binding, protein aggregation-pathway, peptide fibrillation*

A distinctive hallmark of Alzheimer's disease (AD) is the aggregation of amyloid-beta (Aβ) peptides into fibrils and amyloid plaques.[1−3] After being cleaved from the transmembrane amyloid precursor protein (APP),[4] the 39−43 residue long Aβ peptides preferably adopt a random coil structure in solution.[5] Relocated to a membrane environment, they may adopt an α-helical structure,[6] while aggregated fibrils consist of stacked Aβ peptides in parallel β-sheet structure.[7,8] The mechanisms behind these structural transitions are still unclear. During the aggregation process, various intermediate oligomeric assemblies of Aβ peptides are formed, and evidence is building that such oligomers are the toxic species involved in AD pathology.[9−11] However, much still remains to be understood about (Aβ) peptide toxicity, aggregation, and interaction with small molecules such as lipids, drugs, proteins, and ions.

The negatively charged N-terminus of the Aβ peptide binds metal ions like copper(II) and zinc(II) with high affinity.[12−16] Such binding promotes peptide aggregation and alters the aggregation pathways.[17−19] Hence, as elevated levels of copper and zinc have been found in brains of AD patients,[20,21] metal ions may play a role in Alzheimer's disease progression. But also positively charged polyamines such as spermine, spermidine, and their precursor putrescine (Supporting Information Figure S1) display abnormal distribution patterns in brains of AD patients. One study reported that the spermidine levels were increased by 70% in the temporal cortex of AD-affected brains, while the levels of spermine and putrescine were decreased by, respectively, 28% in the temporal cortex and 35% in the occipital cortex.[22−25] Polyamine metabolism furthermore becomes up-regulated in the presence of Aβ peptides.[26] This raises the question whether charged polyamines could interact with Aβ peptides and/or be involved in AD disease progression.

The natural polyamines are small and flexible multivalent cationic alkylamines (Supporting Information Figure S1) that are essential for eukaryotic cell growth. The normal cellular concentrations are around 1 mM for spermine ($C_{10}H_{26}N_4$), and

Received: September 30, 2012
Accepted: December 26, 2012
Published: January 16, 2013

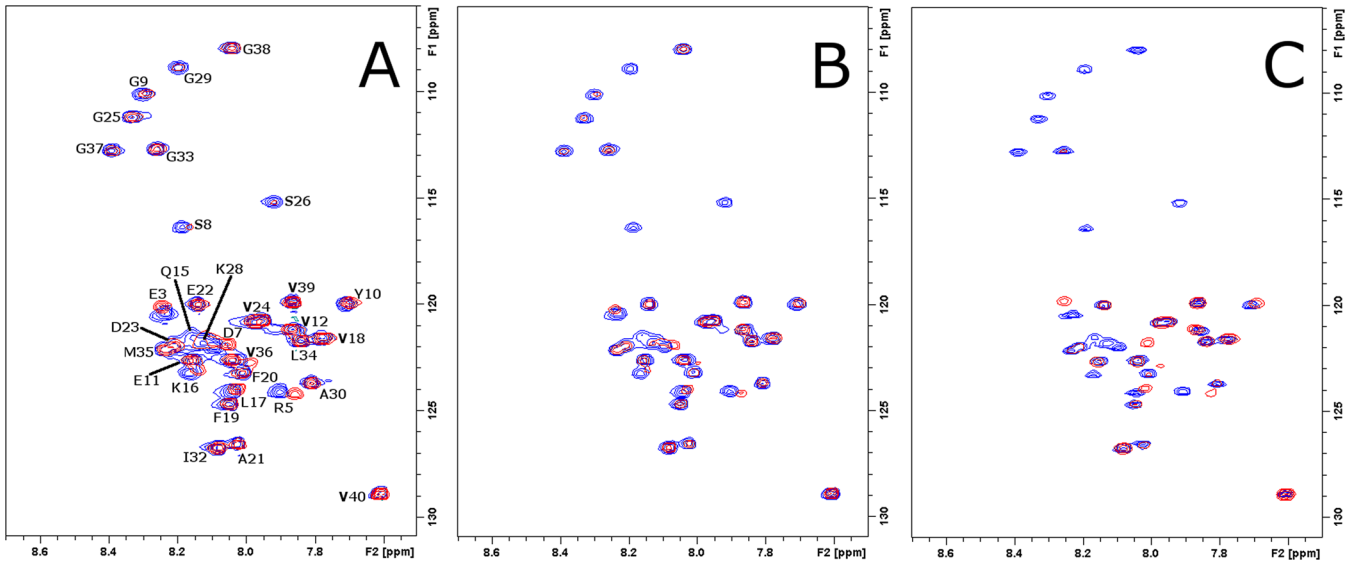

Figure 1. $^{1}H-^{15}N$-HSQC amide region spectra at 5 °C of 100 μM ^{15}N-labeled Aβ(1−40) peptide in 20 mM sodium phosphate buffer at pH 7.3, before (blue) and after (red) addition of 200 μM polyamine: (A) putrescine, (B) spermidine, and (C) spermine.

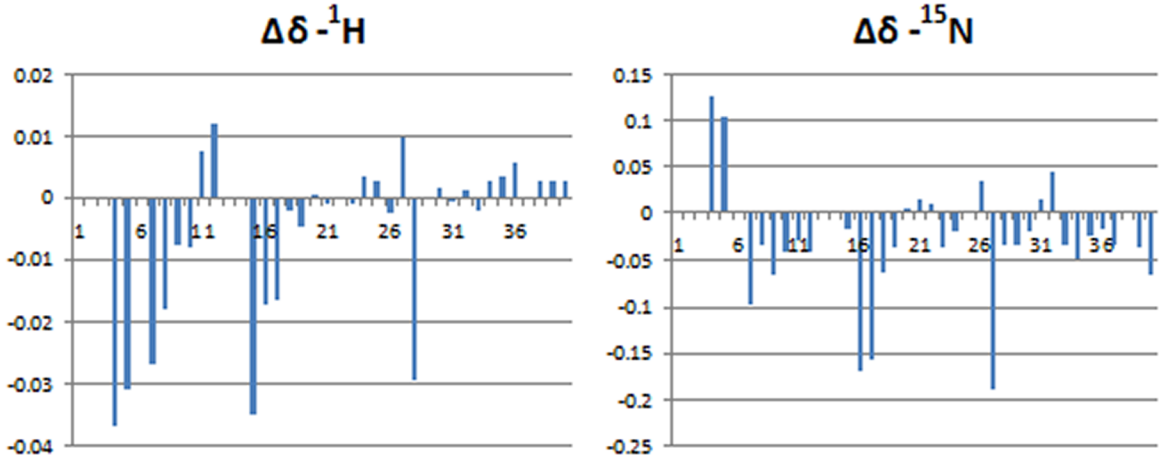

Figure 2. NMR chemical shift differences in $^{1}H-^{15}N$-HSQC spectra at 5 °C of 100 μM ^{15}N-labeled Aβ(1−40) peptide in 20 mM sodium phosphate buffer at pH 7.3, after addition of 200 μM spermidine and evaluated from the data in Figure 1.

slightly higher for spermidine ($C_7H_{19}N_3$) and putrescine ($C_4H_{12}N_2$).[27] At physiological pH the polyamines appear fully protonated, displaying charges of +2 for putrescine, +3 for spermidine, and +4 for spermine.[28] Through interactions with negatively charged regions of DNA, RNA, and proteins, the polyamines regulate gene expression,[29] promote cell migration,[30] and affect the organism's resistance to stress and infectious diseases.[30−32] Cancer cells often display dysregulated polyamine metabolism,[33] and inhibition of polyamine synthesis has been shown to break down the actions of known oncogenes. For these reasons, drugs have been developed that target polyamine metabolism. One example is 2-difluoromethylornithine (DMFO), a specific inhibitor of ornithine decarboxylase (ODC) for regulating putrescine, which has proven effective in the treatment of certain hyperproliferative and infectious diseases.[34]

Polyamines are localized inside and outside of cells, as well as in the plasma membrane.[35,36] The localization of the Aβ peptides in relation to their role in the development of AD pathology has been the subject of debate. Even though the extracellular senile plaques have Aβ as their major constituent, recent work suggests that intracellular Aβ has an important role for the formation of amyloid material.[37,38] It therefore appears likely that polyamines and Aβ have several potential interaction sites in vivo, particularly in cellular organelles, in the cytoplasm, and inside neuronal cells. Neuron degeneration is of course what ultimately makes AD fatal, and polyamines regulate important specific receptor−ligand interactions in the neuronal cells. For example, polyamines activate *N*-methyl-D-aspartate (NMDA) receptors and block the AMPA receptor.[39] The observation that polyamines promote aggregation of the α-synuclein protein involved in Parkinson's disease[27] demonstrates that polyamines can modulate also neurodegenerative disease processes. Consequently, it has been suggested that polyamines could aggravate the neuronal damage associated with AD.[22] In vitro studies of polyamine−Aβ interactions may therefore be important for understanding some of the basic mechanisms of AD pathology.

In this work, we used circular dichroism (CD) and NMR spectroscopy, kinetic thioflavin-T (ThT) measurements via fluorescence spectroscopy, atomic force microscopy (AFM) imaging, and molecular dynamics (MD) and docking

dx.doi.org/10.1021/cn300170x | ACS Chem. Neurosci. 2013, 4, 454−462

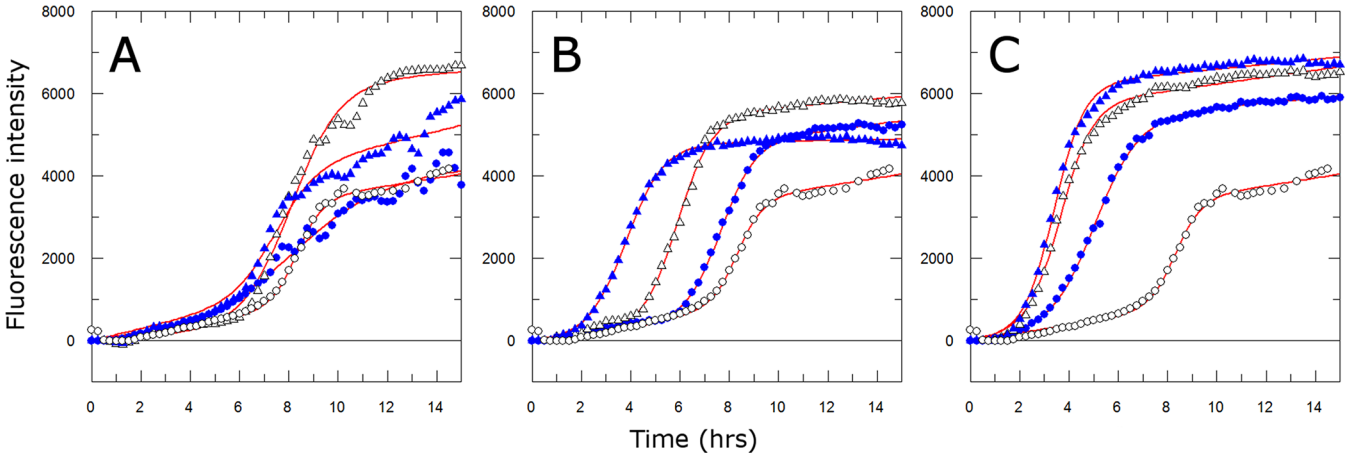

Figure 3. ThT fluorescence assays describing amyloid formation kinetics of 10 μM Aβ(1−40) peptide in the presence of 0 μM (white circles), 10 μM (black circles), 100 μM (white triangles), and 500 μM (black triangles) polyamines, measured in a 50 mM Tris buffer at pH 7.4 and +37 °C: (A) putrescine, (B) spermidine, and (C) spermine.

Table 1. Lag Time (t_{lag}) and Transition Time (t_{trans}) for Amyloid Formation Kinetics of 10 μM Aβ(1-40) Peptide in the Presence of 0, 10, 100, or 500 μM Polyamines (putrescine, spermidine, or spermine), Measured in 50 mM Tris Buffer at pH 7.4 and +37 °C[a]

		putrescine			spermidine			spermine		
	Aβ(1−40) only	10 μM	100 μM	500 μM	10 μM	100 μM	500 μM	10 μM	100 μM	500 μM
lag time, t_{lag} (h)	4.9 ± 2.1	4.7 ± 2.3	4.4 ± 2.1	4.2 ± 1.8	4.5 ± 1.9	3.3 ± 1.3	2.1 ± 0.6	2.5 ± 0.8	1.9 ± 0.4	1.9 ± 0.4
transition time, t_{trans} (h)	7.1 ± 3.2	8.2 ± 3.7	7.5 ± 3.2	6.6 ± 2.4	7.0 ± 2.7	5.9 ± 1.7	4.5 ± 1.2	5.5 ± 1.8	4.2 ± 1.1	4.1 ± 0.8

[a]The t_{lag} and t_{trans} times were obtained from fitting eq 1 (see Methods) to ThT fluorescence assays.

simulations to investigate the interactions between the monomeric Aβ(1−40) peptide and the three polyamines spermine, spermidine, and putrescine, and to monitor the effects of these three polyamines on Aβ peptide aggregation and fibrillization.

RESULTS

NMR Spectroscopy. In order to slow down the aggregation process and allow studies of monomeric Aβ(1−40) peptide, the NMR experiments were performed at low temperature and without agitation. The ^{1}H−^{15}N-HSQC NMR spectra of ^{15}N-labeled Aβ(1−40) before and after addition of polyamines (Figure 1) demonstrate clear differences in amide chemical shifts and decreased cross-peak intensities, proving that all three polyamines bind to the monomeric Aβ(1−40) peptide with fast exchange on the NMR time scale. In particular, the amide cross-peaks of Aβ residues 4−7, 15−17, and 27−28 display significant chemical shift changes in the presence of polyamines, indicating specific interactions at these three locations (Figure 2 and Supporting Information Figure S2). The chemical shift changes do not display any pattern typical for induction of well-ordered secondary structures, such as α-helical or β-sheet conformations. Because the three polyamines induce strikingly similar chemical shift changes, they all appear to interact with the Aβ peptide in a similar manner. The Aβ/polyamine interaction is further supported by the chemical shift changes induced in the 1D NMR spectra of the polyamines when Aβ(1−40) is added (Supporting Information Figure S4). From the NMR data, it is not possible to tell if the polyamines bind with a 1:1 ratio, or if several polyamines bind to different loci on the same Aβ molecule. The NMR spectra did not change upon addition of excess EDTA (data not shown), indicating that the observed effects are not caused by contamination of metal ions. The tetravalent spermine molecule appears to be the strongest binder, as it induces the largest chemical shift changes for a given polyamine concentration (Figure 1). After addition of large amounts of polyamines most Aβ(1−40) amide crosspeaks have lost their intensities, save for V40 (Supporting Information Figure S3). This suggests that the Aβ peptide monomers have aggregated into a state where only this nonbound residue remains flexible enough to show a strong NMR signal. Similar aggregated states with flexible C-termini have previously been observed in studies of Aβ interaction with various small molecules.[40]

Thioflavin T Kinetic Assay. Thioflavin T (ThT) fluorescence is considered a very sensitive marker for the amyloid state of various aggregating proteins and peptides, as ThT in solution displays weak fluorescence in its free form but strong fluorescence when bound to aggregated amyloid fibrils.[41] However, the mechanism of ThT binding to amyloidogenic aggregates is not fully understood, and false positive results have been reported.[42] Thus, ThT binding studies are best used in combination with other results. Here, ThT kinetic fluorescence assays were performed to investigate the effect of different concentrations of the three polyamines on Aβ(1−40) amyloid formation. The resulting kinetic fluorescence curves, obtained using partially agitating conditions, are shown in Figure 3. Lag and transition times, calculated from eq 1, are shown in Table 1. All three polyamines promote aggregation of the Aβ(1−40) peptide, with spermine being the most efficient and putrescine the least efficient promotor. For 10 μM of free Aβ(1−40) peptide, the lag time is 4.9 h and the transition time

dx.doi.org/10.1021/cn300170x | ACS Chem. Neurosci. 2013, 4, 454−462

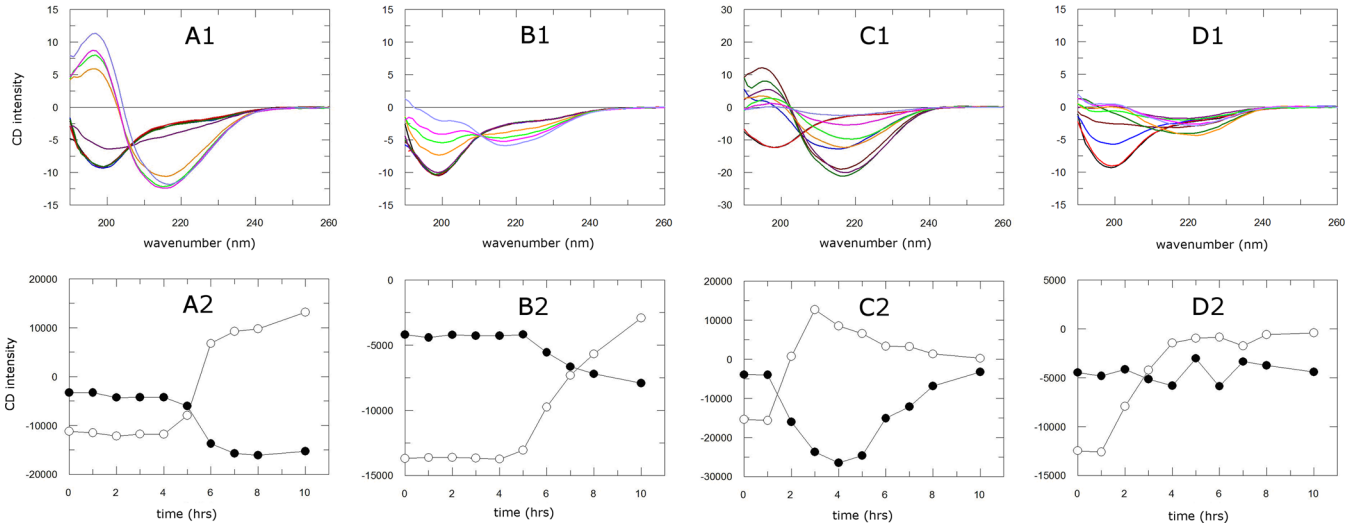

Figure 4. CD data describing kinetics of secondary structure transitions of 10 μM Aβ(1−40) peptide in a 20 mM sodium phosphate buffer at pH 7.3 and 37 °C, after 0, 1, 2, 3, 4, 5, 6, 7, 8, and 10 h incubation with 100 μM of added polyamine: (A) no polyamines, (B) putrescine, (C) spermidine, and (D) spermine. Row 1 shows recorded CD spectra, while row 2 shows CD intensities at 198 nm (open circles) and 216 nm (filled circles) plotted versus time.

is 7.1 h under the present conditions. After addition of 10−500 μM spermine, the lag time becomes around 2 h, and the transition takes 4−5 h (Table 1; Figure 3C). For spermidine, the lag time remained virtually unchanged after a 10 μM addition, but decreased to 3 h in presence of 100 μM spermidine, and to 2 h after addition of 500 μM spermidine (Table 1; Figure 3B). The transition times show a similar concentration-dependency, decreasing from 7 h for pure Aβ peptide to 6 h with 100 μM spermidine and to 4.5 h with 500 μM spermidine. Again, adding only 10 μM spermidine had no significant effect. For putrescine, the effects are very modest, as the 10, 100, and 500 μM additions decrease the lag time from 4.9 h to, respectively, 4.7, 4.4, and 4.2 h. The transition times change by respectively +1.1, +0.4, and −0.5 h. Thus, the lower putrescine concentrations actually seem to prolong the fibrillization process (Table 1; Figure 3A). Control experiments showed that addition of EDTA did not shift the ThT fluorescence curves (Supporting Information Figure S5), nor did the polyamines themselves increase the ThT fluorescence in absence of Aβ peptide (data not shown). Measurements in presence of 0.1−100 mM NaCl confirmed previous results[43] that salt concentration to some extent affects amyloid formation and the corresponding ThT curves. However, the effects induced by the polyamines are too large to be explained by changes in ionic strength alone (Supporting Information Figure S6).

CD Spectroscopy. CD spectroscopy was used to monitor the kinetics of the secondary structure conversions of 10 μM Aβ(1−40) peptide at 37 °C during 10 h, both in the absence and presence of polyamines (100 μM putrescine, spermidine, or spermine). In Figure 4, CD spectra obtained using partially agitating conditions and recorded with 1 h intervals are shown. At time zero, the Aβ(1−40) peptide displays a random coil CD spectrum, with a distinct negative peak around 198 nm. In the absence of polyamines, the CD spectrum gradually adopts a different shape with a positive peak emerging around 197 nm and a negative peak around 216 nm (Figure 4A). The CD signals at 198 and 216 nm are shown as a function of time in Figure 4, demonstrating that the structural transition for free Aβ(1−40) begins after ca. 4 h, and is completed after ca. 6 h. The final spectrum is characteristic of an antiparallel β sheet structure, and the isodichroic point around 206 nm indicates a 1:1 structural transition. These results are in line with previous research, as beta sheets are known to be the building blocks of aggregated Aβ fibrils.[7]

In the presence of 100 μM putrescine, a similar behavior is observed (Figure 4B). After 4 h, the random-coil Aβ peptide slowly starts to adopt a conformation characterized by two positive peaks around 194 and 204 nm, and two negative minima around 216 and 224 nm. Such a spectrum might result from a heterogeneous secondary structure, possibly involving a mixture of parallel and antiparallell beta sheets, with minima around respectively 215 and 222 nm, and perhaps even containing some α-helix conformation with minima at 208 and 222 nm.[44,45] This result indicates that the Aβ peptide with bound putrescine converts into a different secondary structure than the pure Aβ(1−40) peptide. The isodichroic point at 210 nm indicates a general 1:1 transition, which appears not to be fully completed even after 10 h, suggesting slow structural conversion when putrescine is present.

Addition of 100 μM spermidine, on the other hand, induces a rapid structural change that begins after 1 h and ends after 3−4 h (Figure 4C). In the presence of spermidine, the Aβ peptide is converted into a structure displaying a positive CD peak around 196 nm and a negative peak around 216 nm (Figure 4). This appears to be the same antiparallel β-sheet structure as that formed by Aβ(1−40) alone. The 1:1 transition is evidenced by the isodichroic point at 206 nm. After 4 h, the CD spectrum no longer changes its shape, but the CD signal instead grows weaker, most likely a result of peptide aggregation.

Figure 4D shows the kinetic behavior of Aβ(1−40) in the presence of 100 μM spermine. Again a structural transition is observed, yielding a CD spectrum with a positive peak around 203 nm and a negative peak with two minima around 216 and 224 nm. This resulting spectrum is similar to the putrescine-induced CD spectrum, suggesting that the two polyamines induce similar secondary structures in Aβ(1−40). The structural change is very fast: it begins after 1 h and is completed after 4 h, after which the CD spectrum starts to lose signal intensity, most likely a result of peptide aggregation.

dx.doi.org/10.1021/cn300170x | ACS Chem. Neurosci. 2013, 4, 454−462

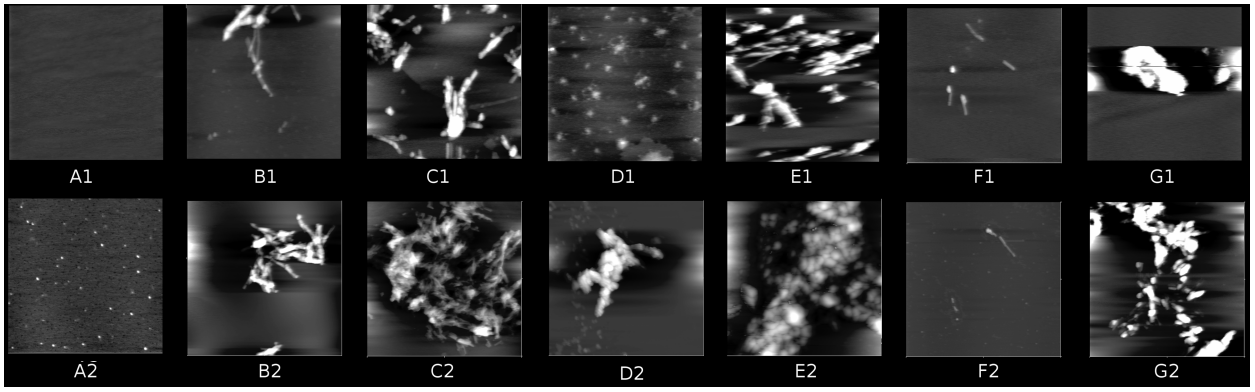

Figure 5. Scanning force microscopy images of aggregated Aβ(1−40) peptides, after 6 h (row 1) or 24 h (row 2) of room temperature incubation in 50 mM TRIS buffer at pH 7.4 and different amounts of added polyamines: (A) no polyamines, (B) 25 μM putrescine, (C) 125 μM putrescine, (D) 25 μM spermidine, (E) 125 μM spermidine, (F) 25 μM spermine, and (G) 125 μM spermine. Each image measures 2 × 2 μm.

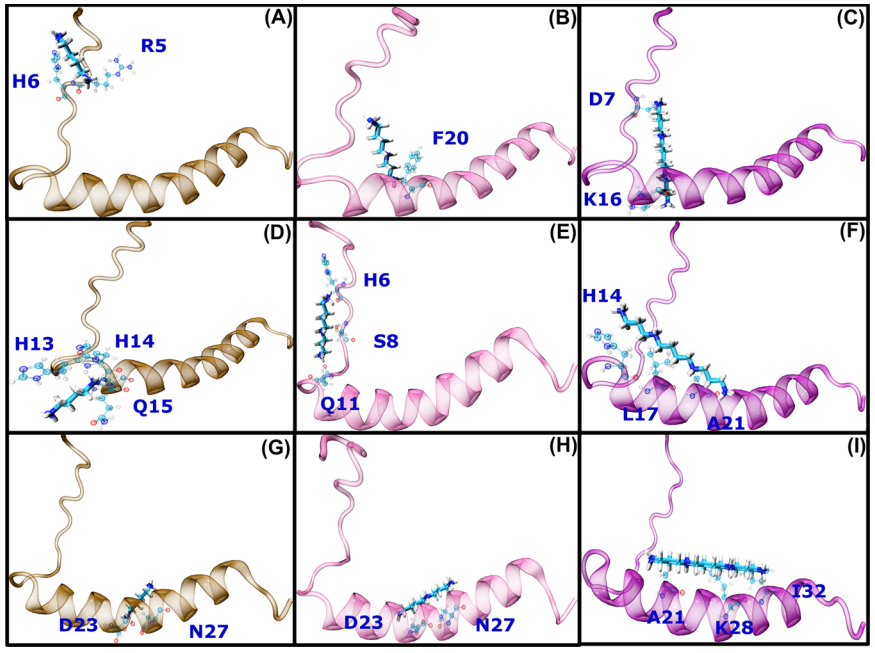

Figure 6. Different possible conformations of the Aβ(1−40) peptide in complex with putrescine (A, D, and G), spermidine (B, E, and H) and spermine (C, F, and I), after 10 ns of MD simulation. Initial structures were obtained by docking using the HEX docking server.[59] Shown here are different conformations of the polyamines complexed with the same isoform of Aβ(1−40) from the NMR fits, and a number of key interactions have been highlighted (see main text for further interaction details). Coordinates of 27 runs using three different conformations of each of three polyamines and three different isoforms of the peptide are provided in the Supporting Information, as are coordinates of the relaxed uncomplexed form of the peptide for all nine computationally amenable isoforms provided in the NMR fit.

Thus, both the structural conversion and the peptide aggregation processes seem to occur at an enhanced rate when spermine is present, and it is likely that both processes take place in parallel, which might explain why no isodichroic point is observed.

AFM Measurements. Atomic force microscopy (AFM) was used to examine the morphologies of the aggregated Aβ peptides, as different aggregation pathways seem to produce different fibril structures that may vary in length, width, curvature, and so forth.[9,27] In Figure 5, we show AFM images of Aβ(1−40) peptides that have fibrillated either alone (Figure 5A) or in the presence of different polyamines (Figure 5B−G). The aggregation products formed in the presence of polyamines clearly display different morphologies compared to the Aβ(1−40) peptides aggregated in Tris buffer only, where no aggregates were observed after 6 h and small globular aggregates had formed after 24 h (Figure 5A). In the presence of putrescine, the Aβ(1−40) peptides form a large number of extensively cross-linked thin fibrils (Figure 4B and C). As expected, the fibril formation increases with time and putrescine concentration. When 25 μM spermidine is present, the Aβ(1−40) peptides form large globular, possibly oligomeric, aggregates after 6 h, which assemble into a cluster after 24 h incubation (Figure 5D). In the presence of 125 μM spermidine, similar clusters of globular aggregates form already after 6 h and grow into large cluster networks after 24 h (Figure 5E). Addition of 25 μM spermine yields formation of thin, smooth, and isolated fibrils already after 6 h (Figure 5F1). After 24 h, these isolated fibrils display little change, except for having grown somewhat longer (Figure 5F2). At the same, time small globular aggregates of the same kind that are observed for Aβ(1−40) alone can be observed (Figure 5F2; cf. A2). The

dx.doi.org/10.1021/cn300170x | ACS Chem. Neurosci. 2013, 4, 454−462

aggregation in the presence of a higher spermine concentration, 125 μM, is markedly different. Now very large amorphous aggregates are formed already after 6 h, and after 24 h the aggregation is even more massive (Figure 5G).

Molecular Dynamics Simulations. Molecular dynamics simulations were used to explore the interactions between monomeric Aβ(1−40) and the three polyamines. Our CD data indicate that the presence of polyamines triggers structural transitions in the Aβ(1−40) peptides on time scales spanning several hours. Such time scales are clearly beyond the scope of computer simulations. We can therefore only study the initial interactions between polyamines and the soluble peptide, in the hope that this might provide clues for the very first steps of the aggregation process. Thus, a relatively short simulation time of 10 ns was deemed sufficient to monitor these initial interactions.

Figure 6 shows the resulting structures after 10 ns simulations of Aβ(1−40) in complex with either putrescine, spermidine, or spermine. All three polyamines appear to preferentially interact with N-terminal residues, and also with some of the central and more ordered charged helical residues such as D23. Three representative structures from the docking ensemble are shown for each isoform, with key interacting residues highlighted in the figure. The coordinates of the corresponding structures for other selected isoforms of the peptide are presented in the Supporting Information. All nine presented structures were stable after 10 ns of simulation at 300 K when only neutralizing counterions were added (Figure 6). When the ion concentration was increased, a gradual unraveling of the helix around residues 23 and 27 was observed already after 10 ns. This unraveled region corresponds to the flexible hinge region when the Aβ peptide adopts a hairpin structure (see discussion section below). The Aβ central helix has previously been shown to completely unfold at 360 K during the course of 20 ns simulation runs,[46] while staying stable at lower temperatures, suggesting that the observed stability would not necessarily be maintained over much longer simulation time scales (running the simulation at higher temperature serves to accelerate potential conformational transitions).

In our simulations, we see hydrogen bonding between Aβ Lys16 and Asp1 and Glu3 in the absence of polyamines, which appears to be important for the structure (Supporting Information Figure S8 and S9). These hydrogen bonds are disrupted by the binding of the polyamines, which show a preference for forming hydrogen bonding interactions with charged Aβ residues such as Asp1, Glu3, Asp7 and Asp23, as well as also interacting with Arg5, His6, Ser8, Tyr10 and Lys16. These results tie in with the observation of significant NMR chemical shifts for residues 4−7, 15−17, 23 and 27−28, even though the MD data did not indicate interactions between the polyamines and Aβ residues 27−28. In the absence of polyamines, two of our three neutralizing Na^+ counterions demonstrated a tendency to move toward the N-terminus: one interacted with His6, Asp 7, and Ser8, and the other with Asp1, Glu3, and Lys16. This position is then replaced by the polyamines, an observation in line with recent reports showing that the major binding site for metal ions like copper and zinc is located in the Aβ N-terminus.[14,47,48]

DISCUSSION AND CONCLUSIONS

In this study, we showed that the three polyamines spermine, spermidine, and putrescine interact with and promote the fibrillation of Aβ(1−40) peptides. Kinetic studies with ThT and CD spectroscopy demonstrated significantly faster structural transitions and aggregation of the AB peptide in presence of the polyamines; the largest effects were seen for spermine, and the smallest for putrescine (Figure 3 and 4; Table 1). The CD measurements suggest that, in the presence of spermidine, the monomeric Aβ(1−40) peptides first convert from a random coil to an antiparallel β-sheet structure and then aggregate in this β-sheet form. This is compatible with previous observations that Aβ peptides in hairpin β-sheet form constitute the building blocks of aggregated Aβ amyloid fibrils. After addition of putrescine and spermine, the Aβ peptides adopt different − and possibly heterogeneous − secondary structures of β-sheet or even α-helix type before aggregating. These different pathways induced by the different polyamines are confirmed by the AFM imaging, which revealed different aggregation products in presence of the three different polyamines.

NMR spectroscopy demonstrated that all three polyamines bind to the monomeric Aβ(1−40) peptide, displaying fast exchange on the NMR time scale. This suggests weak binding, with probable K_D values in the millimolar range. The three polyamines induced similar chemical shift changes in the HSQC amide spectrum of the Aβ peptide, suggesting common specific binding sites around residues 4−5, 15−17, and 27−28. This is in agreement with the computational data, which also indicates binding sites in the central and N-terminal parts of the peptide (Figure 6).

Because the Aβ peptide at neutral pH contains three positively charged and six negatively charged residues (excluding the charged termini), most of which are located in the N-terminal and the middle part of the peptide, electrostatic interaction between these regions and the positively charged polyamines appears likely. Indeed, the MD simulations show formation of hydrogen bonds between the polyamines and many amino acids in these regions, including the negatively charged residues Glu3, Asp7, Glu22, and Asp23. However, as the NMR data indicate specific interactions with residues 15−17 and 27−28 rather than the charged Glu22 and Asp23, electrostatic attraction alone is not sufficient to explain all binding interaction. The polyamines bind to an N-terminal region known to be the binding site for metal ions like Cu(II) and Zn(II), suggesting that in vivo the polyamines might compete with metal ions for binding to the Aβ peptide. This possibility is corroborated by the computational results, which show that the added polyamines compete out a bound sodium ion upon binding to the N-terminus. As metals such as Cu(II) bound to Aβ may contribute to the toxic mechanisms behind AD, possibly by combining redox reactions involving O_2 with differentially promoting and modulating aggregation pathways, binding competition between metal ions and charged polyamines could be a factor affecting AD progression. Other molecules also compete for binding to the Aβ N-terminus, such as apolipoprotein E, where charged residue interactions may lead to a structural rearrangement that renders the protein incapable of performing amyloid beta peptide clearance.[49]

However, polyamines binding to the Aβ N-terminus or elsewhere does not in itself explain why Aβ aggregation would be promoted. Monomeric Aβ is mainly unstructured in aqueous solution,[5] and a first step in Aβ aggregation may be the transient formation of monomeric β-hairpins, which are prone to self-assemble. The Aβ peptide can readily form an intramolecular hairpin with central and C-terminal segments as legs, as demonstrated by solid-state NMR on Aβ(1−42)

fibrils[7,8] and by solution NMR on Aβ(1−40) in complex with an engineered affibody molecule.[50,51] This conformation is further supported by solution NMR studies showing a general tendency for structure induction in the central and C-terminal segments of Aβ.[52,53] The exact residues involved in the β-strand formation varies between the reports, and may even vary depending on the sample conditions. A reasonable estimate is that residues 17−23 and 29−36 comprise the legs of the hairpin, while residues 24−28 constitute the connecting hinge region. Two hypothetical structure-altering mechanisms by the polyamines then appear feasible: the polyamines may interact with the core Aβ fragment and increase the stability of the central region (as was observed in MD simulations of the binding of Pep1B and Dec-DETA to Aβ),[54] or the polyamines may bind to the N-terminal and "pull" on the core fragment, thus facilitating formation of the hairpin. Especially spermine, with its higher charge and longer sequence of aliphatic hydrocarbon chains, should be able to interact both with the central and the N-terminal region (cf. Figure 6C and F), and perhaps this is why spermine promotes Aβ aggregation more efficiently than spermidine and putrescine. On the other hand, the existence of multiple polyamine binding sites on the Aβ(1−40) peptide, observed in the NMR results (Figure 1 and 2) and supported by the MD simulations (Figure 6), raises the question whether one Aβ peptide may bind multiple polyamines (or vice versa). Hence, it is possible that the molecular mechanisms behind the observed polyamine effects cannot be explained from monomeric interactions alone. Elucidating precise structural effects via molecular simulations of multiple polyamines and multimeric forms of the Aβ peptide in varying stoichiometry is however out of the scope of the present work. Addition of polyamines furthermore increases the molecular crowding in the sample, thereby possibly modulating the amyloid formation process.[55] Although the crowding is low under the employed in vitro conditions, it cannot be ruled out that increased crowding, due to polyamines and/or other molecules, affects the Aβ aggregation pathways in vivo.

Our present results provide atomic-level insight into the structural dynamics of the Aβ peptide/polyamine interactions, which helps to explain how the three different polyamines can promote different aggregation pathways of the Aβ peptide. These differential aggregation-facilitating mechanisms are particularly important in light of recent evidence showing that the toxic species in Alzheimer's disease is not the aggregated fibrils, but rather the intermediate oligomers.[9−11] As different intermediate states show varying levels of toxicity, the observed modulation of the aggregation pathways by the naturally occurring polyamines remind us that the key to fighting Alzheimer's disease might not be to prevent Aβ aggregation per se, but to direct the aggregation toward a minimally toxic path.[56]

METHODS

Aβ(1−40) Peptide Preparation. Spermine, spermidine, and putrescine were purchased from Sigma Inc. The 40 aa long amyloid-β peptide Aβ(1−40) was bought either unlabeled or ^{15}N-labeled from AlexoTech AB (Umeå, Sweden) and prepared according to previously described protocols.[47]

Thioflavin T (ThT) Fluorescence Assays. A 10 mM ThT stock solution was prepared in 50 mM tris buffer pH 7.4 and filtered to remove ThT particles. To aliquots of this solution was added polyamines in suitable amounts, and last freshly prepared Aβ(1−40) peptide, yielding final samples containing 5 μM ThT, 10 μM Aβ(1−40), 50 mM Tris buffer, and 10, 100, or 500 μM polyamine (spermine, spermidine, and putrescine). For some control measurements, 1 mM EDTA was added, while other control experiments were carried out in presence of 0.1−100 mM NaCl. All buffers and samples were prepared on ice. The samples were pipetted into a well-plate with 384 wells, holding 45 μL each. Fluorescence measurements were recorded with an Infinite M1000 PRO microplate reader every 15 min, using excitation and emission wavelengths of 446 and 490 nm, respectively. The plate was held at +37 °C, and the wells were automatically shaken 30 s before each measurement step. Each sample was prepared in duplicate, and average fluorescence signals were calculated after subtracting the baseline fluorescence of control samples without Aβ(1−40) peptide. The fluorescence intensity (I) data were fitted to a sigmoid curve with a sloping baseline, using the equation:

$$I(t) = k_1 t + A/(1 + \exp(-k_2(t - t_{1/2}))) \quad (1)$$

where the parameter k_1 describes the sloping baseline, A is the amplitude, k_2 is the elongation rate constant, and $t_{1/2}$ is the time of half completion of the aggregation process. The lag time (t_{lag}) can then be defined as the intercept between the time axis and the tangent with slope k_2 from the midpoint of the fitted sigmoidal curve, that is, $t_{lag} = t_{1/2} - 2/k$.[57] By similar reasoning, the completion time is $t_{1/2} + 2/k$, and it follows that the total transition time (t_{trans}) is $4/k$.

Circular Dichroism (CD). Circular dichroism (CD) spectroscopy was carried out on 400 μL samples of 10 μM Aβ(1−40) peptide in 20 mM sodium phosphate buffer at pH 7.3, either in the absence or in the presence of 100 μM of one of the polyamines (spermine, spermidine, or putrescine). The samples were put in a 2 mm path-length quartz cuvette with a plastic cap, kept at +37 °C, and subjected to 30 min alternating steps of shaking/nonshaking. During the 30 min of shaking, the cuvettes containing the samples were put on a shaking board operating at 225 rpm and +37 °C. During the 30 min of nonshaking, the cuvettes with the samples were kept inside the CD instrument (a Chirascan CD unit from Applied Photophysics, Surrey, U.K.) at +37 °C, and CD spectra were recorded between 190 and 260 nm. In this fashion, CD spectra were recorded once every hour across a 10 h period.

Atomic Force Microscopy (AFM). Samples of 125 uM Aβ(1−40) peptide were incubated with and without polyamines at room temperature for 6 or 24 h. The samples were then diluted 1:1 with Tris buffer (50 mM at pH 7.4) and kept on freshly cleaved mica for 3 min. The excess liquid was shaken off, and the mica plate with deposited sample was rinsed once with 50 mM Tris buffer (pH 7.4) and dried in a stream of dry nitrogen at room temperature. Specimens were mounted on a Multi-Mode atomic force microscope (Digital Instruments Nanoscope III), and images were collected in tapping mode at frequencies around 70 kHz. The imaging was carried out in air, using silicon cantilevers with an asymmetric tip and a force constant of 3 N/m.

NMR Spectroscopy. A Bruker Avance 500 MHz spectrometer was used to record ^{1}H−^{15}N-HSQC spectra at +5 °C of 100 μM ^{15}N-labeled Aβ(1−40) peptide in 20 mM sodium phosphate buffer at pH 7.3 (90/10 H_2O/D_2O), both in the absence and presence of 200, 300, or 500 μM polyamine (spermine, spermidine, or putrescine). For some control measurements, also 1 mM EDTA was added. The spectrometer was equipped with a triple-resonance cryogenically cooled probe head, and the spectra were referenced to the water signal. All NMR measurements were done at +5 °C to slow down the aggregation process. The assignment of the amide peaks for the Aβ(1−40) peptide is known from previous work.[52]

Computational Protocol. The initial atomic coordinates of the Aβ(1−40) peptide[58] were obtained from the Protein Data Bank, accession code 1BA4. Simulations were performed on the native, uncomplexed, monomeric form of Aβ(1−40) and on the peptide in complex with putrescine, spermidine, and spermine. Best-fit conformations of the peptide were obtained using the HEX docking package,[59] as outlined in the Supporting Information. In both the native, unliganded form of the peptide as well as in the peptide−ligand complexes, all ionizable residues were set to their default ionization states at physiological pH (with the exception of histidines, which were kept neutral), and the total system was neutralized by Na^+ or Cl^- ions

as relevant. For comparison, we also performed simulations on the uncomplexed form of the peptide in the presence of 200 mM NaCl. Ions were added using AmberTools 12, via the CHIMERA software package.[60] Molecular dynamics simulations of 10 ns using a 1 fs time step were performed at 300 K following from a 125 ps equilibration run in which the system was gradually heated from 30 to 300 K. All simulations were performed using the MOLARIS simulation package and the ENZYMIX forcefield.[61] Further simulation details can be found in the Supporting Information.

■ ASSOCIATED CONTENT

Supporting Information

Additional NMR measurements, ThT measurements, and molecular dynamics simulations, as Figures S1−S9. This material is available free of charge via the Internet at http://pubs.acs.org.

■ AUTHOR INFORMATION

Corresponding Author

*(S.K.T.S.W.) Mailing address: Department of Biochemistry and Biophysics, Stockholm University, SE-10691 Stockholm, Sweden. Fax: +46 (0)8 153 679. Tel: +46 (0)8 162 444. E-mail: seb@dbb.su.se. (J.P.A.) Mailing address: Gorlaeus Laboratory, Leiden Institute of Chemistry, Leiden University, 2300RA Leiden, The Netherlands. Tel: +31-71-5274213/4557. E-mail: abrahams@chem.leidenuniv.nl.

Author Contributions

J.L., S.K.T.S.W, J.P.A., and A.G. conceived and designed the experiments. J.L., S.K.T.S.W., C.-H.Y., and H.Y. performed the experiments. J.L., S.K.T.S.W., C.-H.Y., H.Y., J.P.A., and A.G. analyzed the data. R.B. and S.C.L.K. designed and performed the computational studies. J.L. and S.K.T.S.W. wrote the paper with input from all the authors.

Funding

This study was supported by grants from the Swedish Research Council to A.G. and S.C.L.K., by a grant from NWO (TOP.08.B3.014) to J.P.A., and by a research project contract (No. J1-2014) from the Slovenian Research Agency to R.B. S.C.L.K. is an ERC Starting Independent Grant holder.

Notes

The authors declare no competing financial interest.

■ ACKNOWLEDGMENTS

The helpful comments and suggestions of the anonymous reviewers significantly improved the manuscript.

■ REFERENCES

(1) Hardy, J., and Selkoe, D. J. (2002) The amyloid hypothesis of Alzheimer's disease: progress and problems on the road to therapeutics. *Science 297*, 353−356.

(2) Munoz, D. G., and Feldman, H. (2000) Causes of Alzheimer's disease. *Can. Med. Assoc. J. 162*, 65−72.

(3) Chiti, F., and Dobson, C. M. (2006) Protein misfolding, functional amyloid, and human disease. *Annu. Rev. Biochem. 75*, 333−366.

(4) Haass, C., and Selkoe, D. J. (1998) Alzheimer's disease. A technical KO of amyloid-beta peptide. *Nature 391*, 339−340.

(5) Danielsson, J., Jarvet, J., Damberg, P., and Gräslund, A. (2005) The Alzheimer beta-peptide shows temperature-dependent transitions between left-handed 3-helix, beta-strand and random coil secondary structures. *FEBS J. 272*, 3938−3949.

(6) Jarvet, J., Danielsson, J., Damberg, P., Oleszczuk, M., and Gräslund, A. (2007) Positioning of the Alzheimer Abeta(1−40) peptide in SDS micelles using NMR and paramagnetic probes. *J. Biomol. NMR 39*, 63−72.

(7) Paravastu, A. K., Leapman, R. D., Yau, W. M., and Tycko, R. (2008) Molecular structural basis for polymorphism in Alzheimer's beta-amyloid fibrils. *Proc. Natl. Acad. Sci. U.S.A. 105*, 18349−18354.

(8) Luhrs, T., Ritter, C., Adrian, M., Riek-Loher, D., Bohrmann, B., Dobeli, H., Schubert, D., and Riek, R. (2005) 3D structure of Alzheimer's amyloid-beta(1−42) fibrils. *Proc. Natl. Acad. Sci. U.S.A. 102*, 17342−17347.

(9) Chromy, B. A., Nowak, R. J., Lambert, M. P., Viola, K. L., Chang, L., Velasco, P. T., Jones, B. W., Fernandez, S. J., Lacor, P. N., Horowitz, P., Finch, C. E., Krafft, G. A., and Klein, W. L. (2003) Self-assembly of Abeta(1−42) into globular neurotoxins. *Biochemistry 42*, 12749−12760.

(10) Fändrich, M. (2012) Oligomeric intermediates in amyloid formation: structure determination and mechanisms of toxicity. *J. Mol. Biol. 421*, 427−440.

(11) Benilova, I., Karran, E., and De Strooper, B. (2012) The toxic Abeta oligomer and Alzheimer's disease: an emperor in need of clothes. *Nat. Neurosci. 15*, 349−357.

(12) Talmard, C., Bouzan, A., and Faller, P. (2007) Zinc binding to amyloid-beta: isothermal titration calorimetry and Zn competition experiments with Zn sensors. *Biochemistry 46*, 13658−13666.

(13) Atwood, C. S., Scarpa, R. C., Huang, X., Moir, R. D., Jones, W. D., Fairlie, D. P., Tanzi, R. E., and Bush, A. I. (2000) Characterization of copper interactions with alzheimer amyloid beta peptides: identification of an attomolar-affinity copper binding site on amyloid beta1−42. *J. Neurochem. 75*, 1219−1233.

(14) Danielsson, J., Pierattelli, R., Banci, L., and Gräslund, A. (2007) High-resolution NMR studies of the zinc-binding site of the Alzheimer's amyloid beta-peptide. *FEBS J. 274*, 46−59.

(15) Tõugu, V., Karafin, A., and Palumaa, P. (2008) Binding of zinc(II) and copper(II) to the full-length Alzheimer's amyloid-beta peptide. *J. Neurochem. 104*, 1249−1259.

(16) Zawisza, I., Rózga, M., and Bal, W. (2012) Affinity of copper and zinc ions to proteins and peptides related to neurodegenerative conditions (Aβ, APP, α-synuclein, PrP). *Coord. Chem. Rev. 256*, 2297−2307.

(17) Tõugu, V., Tiiman, A., and Palumaa, P. (2011) Interactions of Zn(II) and Cu(II) ions with Alzheimer's amyloid-beta peptide. Metal ion binding, contribution to fibrillization and toxicity. *Metallomics 3*, 250−261.

(18) Miller, Y., Ma, B., and Nussinov, R. (2010) Zinc ions promote Alzheimer Abeta aggregation via population shift of polymorphic states. *Proc. Natl. Acad. Sci. U.S.A. 107*, 9490−9495.

(19) Pedersen, J. T., Ostergaard, J., Rozlosnik, N., Gammelgaard, B., and Heegaard, N. H. (2011) Cu(II) mediates kinetically distinct, non-amyloidogenic aggregation of amyloid-beta peptides. *J. Biol. Chem. 286*, 26952−26963.

(20) Lovell, M. A., Robertson, J. D., Teesdale, W. J., Campbell, J. L., and Markesbery, W. R. (1998) Copper, iron and zinc in Alzheimer's disease senile plaques. *J. Neurol. Sci. 158*, 47−52.

(21) Religa, D., Strozyk, D., Cherny, R. A., Volitakis, I., Haroutunian, V., Winblad, B., Naslund, J., and Bush, A. I. (2006) Elevated cortical zinc in Alzheimer disease. *Neurology 67*, 69−75.

(22) Singh, M., Dang, T. N., Arseneault, M., and Ramassamy, C. (2010) Role of by-products of lipid oxidation in Alzheimer's disease brain: a focus on acrolein. *J. Alzheimer's Dis. 21*, 741−756.

(23) Morrison, L. D., and Kish, S. J. (1995) Brain polyamine levels are altered in Alzheimer's disease. *Neurosci. Lett. 197*, 5−8.

(24) Seidl, R., Beninati, S., Cairns, N., Singewald, N., Risser, D., Bavan, H., Nemethova, M., and Lubec, G. (1996) Polyamines in frontal cortex of patients with Down syndrome and Alzheimer disease. *Neurosci. Lett. 206*, 193−195.

(25) Vivo, M., de Vera, N., Cortes, R., Mengod, G., Camon, L., and Martinez, E. (2001) Polyamines in the basal ganglia of human brain. Influence of aging and degenerative movement disorders. *Neurosci. Lett. 304*, 107−111.

(26) Yatin, S. M., Yatin, M., Varadarajan, S., Ain, K. B., and Butterfield, D. A. (2001) Role of spermine in amyloid beta-peptide-associated free radical-induced neurotoxicity. *J. Neurosci. Res. 63*, 395−401.
(27) Antony, T., Hoyer, W., Cherny, D., Heim, G., Jovin, T. M., and Subramaniam, V. (2003) Cellular polyamines promote the aggregation of alpha-synuclein. *J. Biol. Chem. 278*, 3235−3240.
(28) Bencini, A., Bianchi, A., Garcia-España, E., Micheloni, M., and Ramirez, J. A. (1999) Proton coordination by polyamine compounds in aqueous solution. *Coord. Chem. Rev. 188*, 97−156.
(29) Chattopadhyay, M. K., Chen, W., Poy, G., Cam, M., Stiles, D., and Tabor, H. (2009) Microarray studies on the genes responsive to the addition of spermidine or spermine to a Saccharomyces cerevisiae spermidine synthase mutant. *Yeast 26*, 531−544.
(30) Minois, N., Carmona-Gutierrez, D., and Madeo, F. (2011) Polyamines in aging and disease. *Aging 3*, 716−732.
(31) Hussain, S. S., Ali, M., Ahmad, M., and Siddique, K. H. (2011) Polyamines: natural and engineered abiotic and biotic stress tolerance in plants. *Biotechnol. Adv. 29*, 300−311.
(32) Eisenberg, T., Knauer, H., Schauer, A., Buttner, S., Ruckenstuhl, C., Carmona-Gutierrez, D., Ring, J., Schroeder, S., Magnes, C., Antonacci, L., Fussi, H., Deszcz, L., Hartl, R., Schraml, E., aaCriollo, A., Megalou, E., Weiskopf, D., Laun, P., Heeren, G., Breitenbach, M., Grubeck-Loebenstein, B., Herker, E., Fahrenkrog, B., Frohlich, K. U., Sinner, F., Tavernarakis, N., Minois, N., Kroemer, G., and Madeo, F. (2009) Induction of autophagy by spermidine promotes longevity. *Nat. Cell Biol. 11*, 1305−1314.
(33) Thomas, T., and Thomas, T. J. (2003) Polyamine metabolism and cancer. *J. Cell. Mol. Med. 7*, 113−126.
(34) Sinicrope, F. A., Broaddus, R., Joshi, N., Gerner, E., Half, E., Kirsch, I., Lewin, J., Morlan, B., and Hong, W. K. (2011) Evaluation of difluoromethylornithine for the chemoprevention of Barrett's esophagus and mucosal dysplasia. *Cancer Prev. Res. 4*, 829−839.
(35) Rubinstein, S., and Breitbart, H. (1994) Cellular localization of polyamines: Cytochemical and ultrastructural methods providing new clues to polyamine function in ram spermatozoa. *Biol. Cell 81*, 177−183.
(36) Yatin, M. (2002) Polyamines in living organisms. *J. Cell Mol. Biol. 1*, 57−67.
(37) LaFerla, F. M., Green, K. N., and Oddo, S. (2007) Intracellular amyloid-β in Alzheimer's disease. *Nat. Rev. Neurosci. 8*, 499−509.
(38) Zheng, L., Cedazo-Minguez, A., Hallbeck, M., Jerhammar, F., Marcusson, J., and Terman, A. (2012) Intracellular distribution of amyloid beta peptide and its relationship to the lysosomal system. *Transl. Neurodegener. 1*, 19.
(39) Washburn, M. S., and Dingledine, R. (1996) Block of alpha-amino-3-hydroxy-5-methyl-4-isoxazolepropionic acid (AMPA) receptors by polyamines and polyamine toxins. *J. Pharmacol. Exp. Ther. 278*, 669−678.
(40) Lendel, C., Bolognesi, B., Wahlström, A., Dobson, C. M., and Gräslund, A. (2010) Detergent-like interaction of Congo red with the amyloid beta peptide. *Biochemistry 49*, 1358−1360.
(41) Biancalana, M., and Koide, S. (2010) Molecular mechanism of Thioflavin-T binding to amyloid fibrils. *Biochim. Biophys. Acta 1804*, 1405−1412.
(42) Jameson, L. P., Smith, N. W., and Dzyuba, S. V. (2012) Dye-Binding Assays for Evaluation of the Effects of Small Molecule Inhibitors on Amyloid (Aβ) Self-Assembly. *ACS Chem. Neurosci. 3*, 807−819.
(43) Klement, K., Wieligmann, K., Meinhardt, J., Hortschansky, P., Richter, W., and Fändrich, M. (2007) Effect of different salt ions on the propensity of aggregation and on the structure of Alzheimer's abeta(1−40) amyloid fibrils. *J. Mol. Biol. 373*, 1321−1333.
(44) Tilstra, L., and Mattice, W. L. (1996) The β Sheet to coil transition of polypeptides, as determined by circular dichroism. In *Circular dichroism and the conformational analysis of biomolecules* (Fasman, G. D., Ed.), Plenum Press, New York.
(45) Balcerski, J. S., Pysh, E. S., Bonora, G. M., and Toniolo, C. (1976) Vacuum ultraviolet circular dichroism of beta-forming alkyl oligopeptides. *J. Am. Chem. Soc. 98*, 3470−3473.
(46) Ito, M., Johansson, J., Strömberg, R., and Nilsson, L. (2011) Unfolding of the amyloid beta-peptide central helix: mechanistic insights from molecular dynamics simulations. *PLoS One 6*, e17587.
(47) Ghalebani, L., Wahlström, A., Danielsson, J., Wärmländer, S. K. T. S., and Gräslund, A. (2012) pH-dependence of the specific binding of Cu(II) and Zn(II) ions to the amyloid-beta peptide. *Biochem. Biophys. Res. Commun. 421*, 554−560.
(48) Faller, P., and Hureau, C. (2009) Bioinorganic chemistry of copper and zinc ions coordinated to amyloid-beta peptide. *Dalton Trans.*, 1080−1094.
(49) Luo, J., Marechal, J. D., Wärmländer, S. K. T. S., Gräslund, A., and Peralvarez-Marin, A. (2010) In silico analysis of the apolipoprotein E and the amyloid beta peptide interaction: misfolding induced by frustration of the salt bridge network. *PLoS Comput. Biol. 6*, e1000663.
(50) Hoyer, W., Grönwall, C., Jonsson, A., Ståhl, S., and Härd, T. (2008) Stabilization of a beta-hairpin in monomeric Alzheimer's amyloid-beta peptide inhibits amyloid formation. *Proc. Natl. Acad. Sci. U.S.A. 105*, 5099−5104.
(51) Lindgren, J., Wahlström, A., Danielsson, J., Markova, N., Ekblad, C., Gräslund, A., Abrahmsen, L., Karlström, A. E., and Wärmländer, S. K. (2010) N-terminal engineering of amyloid-beta-binding Affibody molecules yields improved chemical synthesis and higher binding affinity. *Protein Sci. 19*, 2319−2329.
(52) Danielsson, J., Andersson, A., Jarvet, J., and Gräslund, A. (2006) 15N relaxation study of the amyloid beta-peptide: structural propensities and persistence length. *Magn. Reson. Chem. 44*, S114−121.
(53) Yamaguchi, T., Matsuzaki, K., and Hoshino, M. (2011) Transient formation of intermediate conformational states of amyloid-beta peptide revealed by heteronuclear magnetic resonance spectroscopy. *FEBS Lett. 585*, 1097−1102.
(54) Ito, M., Johansson, J., Strömberg, R., and Nilsson, L. (2012) Effects of ligands on unfolding of the amyloid beta-peptide central helix: mechanistic insights from molecular dynamics simulations. *PLoS One 7*, e30510.
(55) Qian, M., Jun-Bao, F., Zheng, Z., Bing-Rui, Z., Sheng-Rong, M., Ji-Ying, H., Jie, C., and Yi, L. (2012) The Contrasting Effect of Macromolecular Crowding on Amyloid Fibril Formation. *PLoS One 7*, e36288.
(56) Seilheimer, B., Bohrmann, B., Bondolfi, L., Muller, F., Stuber, D., and Dobeli, H. (1997) The toxicity of the Alzheimer's beta-amyloid peptide correlates with a distinct fiber morphology. *J. Struct. Biol. 119*, 59−71.
(57) Hellstrand, E., Boland, B., Walsh, D. M., and Linse, S. (2010) Amyloid beta-Protein Aggregation Produces Highly Reproducible Kinetic Data and Occurs by a Two-Phase Process. *ACS Chem. Neurosci. 1*, 13−18.
(58) Coles, M., Bicknell, W., Watson, A. A., Fairlie, D. P., and Craik, D. J. (1998) Solution structure of amyloid beta-peptide(1−40) in a water-micelle environment. Is the membrane-spanning domain where we think it is? *Biochemistry 37*, 11064−11077.
(59) Ritchie, D. W. (2003) Evaluation of protein docking predictions using Hex 3.1 in CAPRI rounds 1 and 2. *Proteins 52*, 98−106.
(60) Pettersen, E. F., Goddard, T. D., Huang, C. C., Couch, G. S., Greenblatt, D. M., Meng, E. C., and Ferrin, T. E. (2004) UCSF Chimera–a visualization system for exploratory research and analysis. *J. Comput. Chem. 25*, 1605−1612.
(61) Lee, F. S., Chu, Z. T., and Warshel, A. (1993) Microscopic and semimicroscopic calculations of electrostatic energies in proteins by the POLARIS and ENZYMIX programs. *J. Comput. Chem. 14*, 161−185.